

DOI: 10.1002/sml.200700600

Visualization of Carrier Depletion in Semiconducting Nanowires**

Oliver Hayden,* Gengfeng Zheng, Prabhat Agarwal, and Charles M. Lieber

Semiconducting nanowires (NWs)^[1] grown by the vapour–liquid–solid (VLS) mechanism are attractive building blocks for nanoscale devices. A central question in the study of such devices is to what degree the physical concepts established to describe larger planar semiconductor devices can be extended to these new NW devices. For instance, the large surface-to-volume ratio in nanoscale devices leads to the electrostatics and transport properties becoming strongly influenced by the surrounding environment and not dependent only on the intrinsic properties of the semiconductor alone.^[2] As the most basic element of many electronic and optoelectronic devices and circuits, p-type/n-type (pn) junction diodes are a useful starting point for the physics of nanoscale devices. It has long been known that nearby dielectrics (and field-shaping electrodes) can enhance the breakdown voltage in planar junctions via a reduction of the maximum surface field.^[3] Similarly, the electric field inside SiO₂-embedded NW pn junctions is smeared out and charge carriers experience a potential landscape controlled by the dielectric environment, which in turn results in even a suppression of avalanche breakdown.^[4] Thus, a technique to directly map the space–charge layer in NWs would be of general interest. Previous work used time-consuming scanning-gate^[5] and near-field scanning optical microscopy techniques^[6] to probe the concentration of charge carriers in NWs.

Here, we report the visualization of the depletion width in crossed NW pn heterojunctions with a far-field optical ex-

periment that can be readily applied to characterize charge-carrier distribution in nanoscale structures. Unlike rather laborious near-field scanning of the space–charge layer width by local illumination of a NW, global low-excitation photoluminescence (PL) of a NW and far-field optical microscopy of the PL are sufficient to probe the charge-carrier separation in NWs.

Crossed-NW devices have been used to demonstrate logic operations,^[7] light-emitting devices^[8] and lab-on-chip applications.^[9] Most recently, crossed-NW devices from n-CdS/p-Si were used as polarization-sensitive photodetectors at room temperature.^[10] Spatially resolved photocurrent measurements revealed the nanoscale pn-junction device as the active area of the photodiodes and by controlling the doping level of the p-Si NWs Zener and avalanche diodes were fabricated. Although the breakdown mechanism is different in both types of diode, differences in carrier concentration across the pn junction always generate a depletion layer with a strong electric field. Due to the large surface-to-volume ratio of NWs a deviation of the nanoscale space–charge layer from bulk diodes can be expected.^[11] We have observed that the breakdown voltage of n-CdS/p⁺-Si crossed-NW diodes cooled down to 4.2 K in an optical cryostat shifts to very high reverse biases (>60 V), which gives us access to extended space–charge layers. PL measurements of crossed p⁺-Si-NW/n-CdS-NW diodes show that the depletion-layer thickness extends over several micrometers in CdS NWs and the width of the space–charge layer can be controlled by the illumination intensity and the reverse bias. Interestingly, these results show that the depletion width does not scale with the square root of the bias voltage but is linearly dependent on the reverse bias and thus suggests unusual carrier distributions in these crossed junctions.

PL measurements of the CdS-NW in n-CdS/p⁺-Si crossed-NW junctions and subsequent analysis of the PL was used to determine details of charge carrier recombination in the active region of the reverse biased pn junction as described below. Figure 1A shows the experimental set up. A defocused laser beam at 400 nm was used to illuminate the device area and to stimulate a uniform PL from the single n-CdS-NW (direct-bandgap material). PL spectra and images were recorded with a home-built epifluorescence microscope and a liquid nitrogen cooled CCD (Princeton Instruments Spec-10). Figure 1B and C shows a scanning electron microscopy (SEM) image of the photodiode and a CCD image of the illuminated device, respectively. Uniform PL with a near-band-edge emission of ≈ 514 nm is observed along the entire CdS NW length. We observe no feature in the PL of the junction at zero bias, which we could identify with an equilibrium depletion region. This indicates a very small value of the built-in voltage at the low temperatures of the experiment, or a spatial extent of the depletion region below the limited resolution of the microscope. No PL is observed at the position of the SiNW, which is an indirect bandgap material. The two dark areas at the ends of the CdS NW correspond to the position of optically opaque top metal contacts. With applied forward bias to the diode electroluminescence (EL) appears right at the pn junction

[*] Dr. O. Hayden
Current address:
SIEMENS AG, Corporate Technology CT MM1
Günther-Scharowsky-Strasse 1
91050 Erlangen (Germany)
Fax: (+49) 91-317-328-04
E-mail: oliver.hayden@siemens.com
Dr. G. Zheng, Dr. C. M. Lieber
Department of Chemistry and Chemical Biology
Harvard University
12 Oxford Street, Cambridge, MA 02138 (USA)
Dr. P. Agarwal
NXP Semiconductors, Research
Kapeldreef 75
3001 Leuven (Belgium)

[**] Fruitful discussions with Dr. Mikael T. Björk and Dr. Ritesh Agarwal are gratefully acknowledged. This work was partially supported by the EU program NODE 015783.



Supporting information for this article is available on the WWW under <http://www.small-journal.com> or from the author.

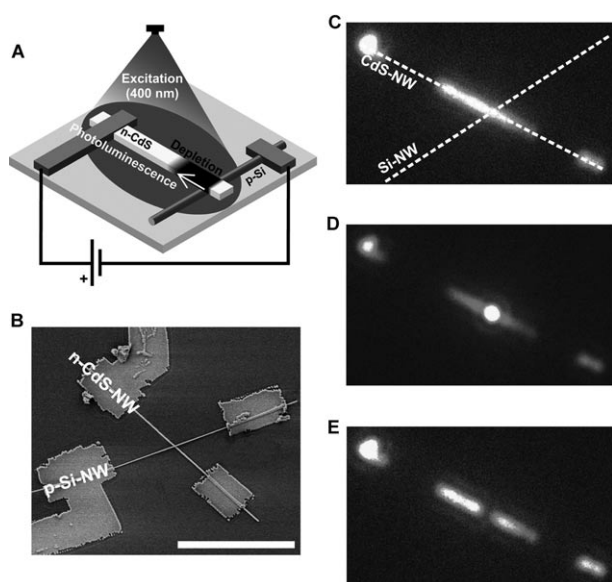


Figure 1. Visualization of carrier depletion at 4.2 K. A) Schematic of the crossed-NW LED with reverse bias applied. A defocused laser spot is used to excite the PL from the CdS NW. B) SEM micrograph of the crossed-NW device (n-CdS/p⁺-Si) with top metal contacts. The scale bar is 10 μm . C) PL of the CdS NW with an excitation of 5.8 W cm^{-2} at 400 nm. D) The NW device at 5 V forward bias with EL from the pn junction. E) The diode with 10 V reverse bias. The contrast level of the PL images of the device with forward and reverse bias is not the same.

(Figure 1D). At reverse bias the PL disappears at the junction (Figure 1E). We note that the PL is unaffected at the metal/semiconductor junction as well as for the unbiased portion of the CdS NW.

With increasing reverse bias the area without PL emission extends from the junction along the CdS NW over several micrometers. In analogy with the well-known “dead-layer” model^[12] for the absence of PL in surface depletion layers, we attribute the observed absence of PL to the presence of a space-charge layer due to a pn heterojunction. In this depletion layer, photogenerated electrons and holes are separated in the junction electric field before they can recombine. Consequently, the region showing PL in the CdS-NW is attributed to a quasineutral region without strong electric fields, allowing the photogenerated carriers to recombine. In this picture, the crossed NWs in our experiment represent a pn heterojunction, and the photoluminescence delineates the depletion region.

Figure 2 shows the depletion width W as a function of voltage V (negative values for reverse bias) at an excitation intensity of $1.7 \times 10^{-2} \text{ W cm}^{-2}$ (400-nm excitation wavelength). At 4.2 K no breakdown was observed up to 65 V reverse bias applied to the diode. The depletion width increases linearly with reverse bias and a constant k of $\approx 0.12 \mu\text{m V}^{-1}$, which is in strong contradiction to three-dimensional (3D) junctions, where one expects a relation between the depletion length and the voltage following square-root dependence. Note the linear fit of the observed space charge layer as well as for the theoretical curves in Figure 2 indicates a \approx zero depletion width at zero reverse bias and thus

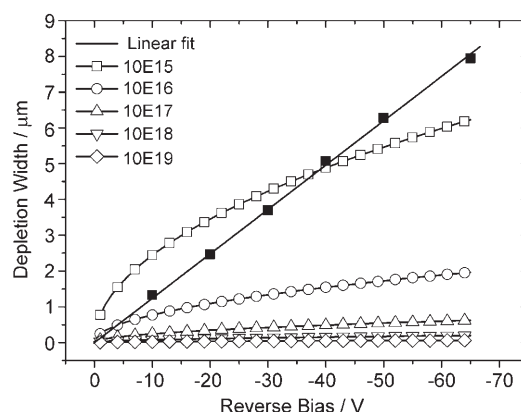


Figure 2. Depletion width in a CdS NW in dependence of the reverse bias voltage applied to the NW pn junction at an excitation level of $1.7 \times 10^2 \text{ W cm}^{-2}$ at 400 nm (filled squares). The space-charge region is extracted from the PL probing experiments. Note the extraction of the depletion width is limited by the optical resolution. Calculated space-charge regions for a 3D diode assuming an abrupt pn junction are shown for a dopant concentration in CdS from 10^{15} to 10^{19} cm^{-3} (open symbols) to illustrate the nonlinear depletion width in the bulk.

a small built-in potential of the heterostructure. The carrier drift length of several micrometers exceeds the reported diffusion lengths of charge carriers and excitons in CdS, which are approximately 0.5 to 1 μm at 7 K.^[13]

$$W_{\text{NW}} = k \cdot |V| \quad (1)$$

In bulk pn junctions the depletion width W_{Bulk} shows a square-root dependency on the applied reverse bias^[14]

$$W_{\text{Bulk}} = \sqrt{\frac{2\epsilon_s(V_{\text{bi}} - V)}{qN_{\text{CdS}}}} \quad (2)$$

with the semiconductor dielectric permittivity ϵ_s (dielectric constant of CdS is 5.4), the built-in potential V_{bi} , the elementary charge q , and the carrier concentration N_{CdS} assuming an abrupt junction. For comparison, calculated space-charge regions of a 3D abrupt n-CdS/p⁺-Si junction with a CdS doping concentration from 10^{15} to 10^{19} cm^{-3} are added to Figure 2. Clear differences of the depletion width in dependence of the reverse bias between the one- and three-dimensional case are observed. With depletion layer widths of 1 to 10 μm a depletion capacitance per unit area of $\approx 5 \times 10^{-9}$ to $5 \times 10^{-10} \text{ F cm}^{-2}$, respectively, can be calculated for the crossed-NW diode.

Unusual voltage dependence of the depletion width and depletion capacitance have been reported for several low-dimensional pn junctions.^[11,15,16] For instance, in the case of 2D planar junctions¹⁵, the junction electric field is concentrated in the environment whereas the charge carriers and the ionized dopants are in the plane of the 2D pn junction. The electric field is weakly screened and thus the depletion region will be extended. For the case of 1D junctions, theoretical calculations have suggested the existence of unusual length scales in carbon-nanotube diodes.^[11] Experimental re-

sults on silicon nanowire diodes have demonstrated the influence of the surrounding dielectric on the electric-field distribution inside the space charge region.^[16] In our case the NW diode in the optical cryostat is not fully embedded in dielectric material but is only partially in contact with the SiO₂-covered substrate. In fact most of the NW surface is in vacuum. Therefore, the electric field for our 1D junctions will be even more weakly screened.

The experimentally derived constant k can be further described by a first-order approximation of the 2D case^[15] to depend linearly on the semiconductor permittivity, the charge-carrier concentration, and a geometrical factor, f .

$$k = f \cdot \frac{\epsilon_s}{qN_{\text{CdS}}}$$

The excitation level of $1.7 \times 10^{-2} \text{ Wcm}^{-2}$ used to probe the photoluminescence in Figure 2 corresponds to approximately a single absorbed photon per laser pulse. In addition, the large surface-to-volume ratio of the CdS NW will result in an enhanced surface recombination of the carriers generated by illumination. We thus can assume a negligible screening of the electrical field by photons absorbed in the CdS NW and extract an estimate of the intrinsic doping concentration of the CdS NW of $\approx 2 \times 10^{15} \text{ cm}^{-3}$ times the geometrical factor f at 4.2 K. In the case of 2D pn junctions f is modeled to be around 1 to 8.^[15]

It is well known that increasing the illumination intensity influences the PL intensity in semiconductors. Additional photogenerated carriers can saturate surface states and, at some level, will screen the junction electric field; thus radiative recombination will be facilitated. Figure 3 shows the PL of an n-CdS/p⁺-Si NW diode with and without applied bias and three illumination levels. The position of the pn junction is highlighted in Figure 3B where the LED emission from the junction is shown at a forward bias of 5 V. With decreasing illumination power the CdS-NW portion reverse-biased at -65 V shows an increase of the space-charge region (Figure 3C–E and Supporting Information). Again, no depletion is observed at the metal/semiconductor junction as well as in the unbiased portion of the CdS NW. Figure 4 summarizes results with varying illumination levels and reverse biases. The linear relationship between reverse bias and the space-charge region is maintained over four orders of magnitude of illumination levels from 0.01 to 100 Wcm^{-2} (Figure 4A). With increasing illumination level the bias dependence of the depletion width decreases exponentially and saturates at a value of around $\approx 0.05 \mu\text{mV}^{-1}$. This observation is consistent with the screening of the electric field by photogenerated carriers (Figure 4B).

In Figure 4C and D the depletion width versus the illumination level is plotted on a linear and a logarithmic scale of four different devices at a reverse bias of 65 V. In addition, the average number of photons getting absorbed in the biased part of the CdS NWs per second is shown in Figure 4D. The exponential decrease of the space charge region shows that at low illumination levels few photogenerated carriers have a dramatic influence on the depletion width whereas at a high concentration of carriers the deple-

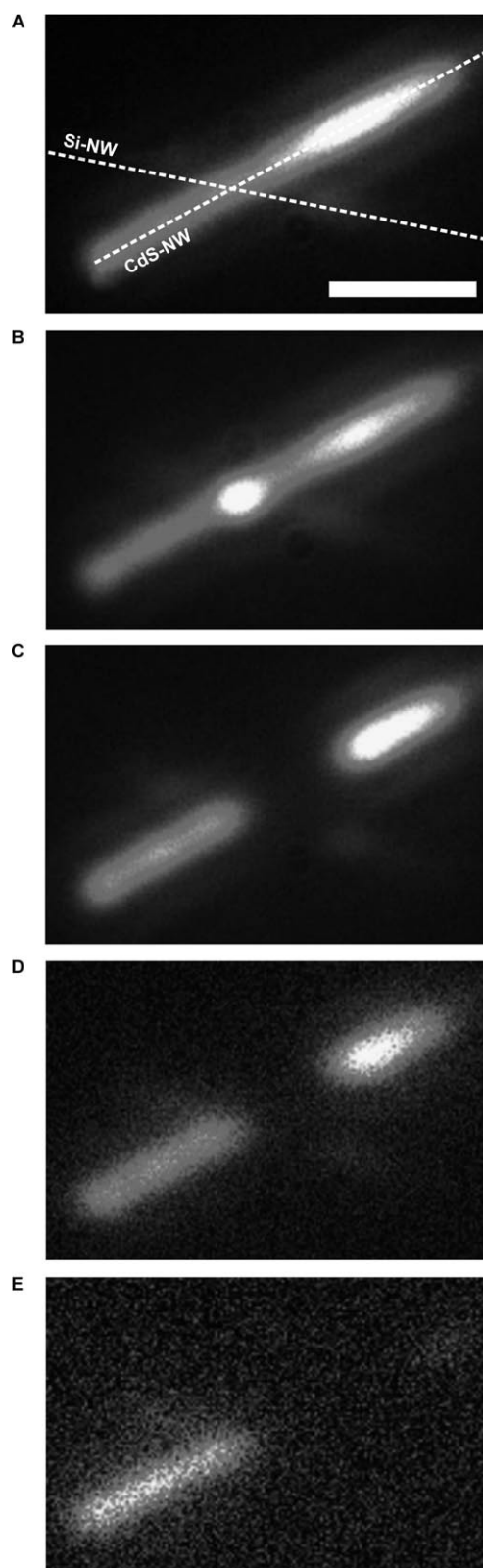


Figure 3. PL images of a crossed-NW photodiode in dependence of the illumination level at 4.2 K. A) The unbiased device at 6.6 Wcm^{-2} . The scale bar is $4 \mu\text{m}$. B) Forward bias of 5 V PL at 6.6 Wcm^{-2} . PL images of the diode reverse biased at 65 V and excited at an illumination level of C) 6.6 Wcm^{-2} , D) 0.6 Wcm^{-2} , and E) 0.13 Wcm^{-2} .

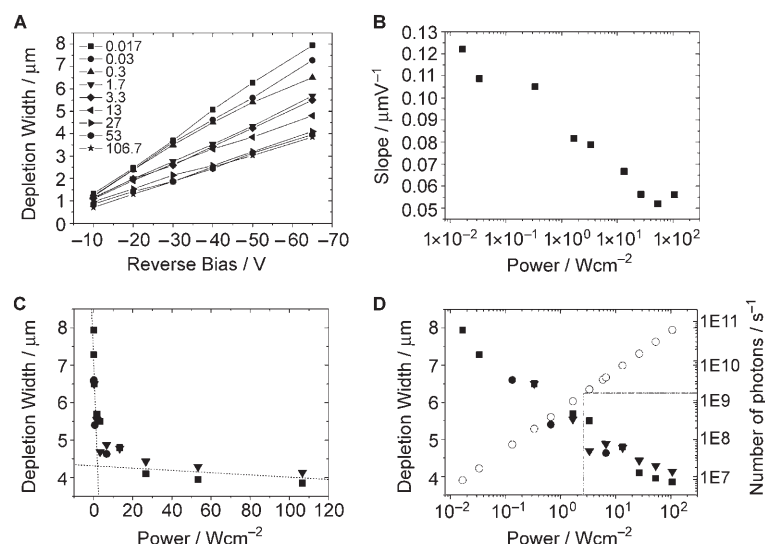


Figure 4. Illumination-level dependence of the depletion width. A) Depletion measured at varying reverse bias and illumination power (Wcm⁻²) at 400 nm. B) The average linear slopes in dependence of the illumination. NW space-charge layers of four different devices versus the illumination intensity on a C) linear and D) logarithmic scale are shown (broken lines are to guide the eye). The average numbers of photons per second absorbed in the fraction of the CdS-NW with applied bias is added.

tion length starts to level off to around 50% of its initial value. At the same time as the illumination level increases the current of the reverse-biased NW diode increases. Above ≈ 1 nA of reverse current the number of charge carriers exceeds the number of photogenerated carriers. In Figure 4C the broken lines correspond to a roughly linear fit of the illumination-dependent and -independent parts of the depletion width plot. The transition steps in around an illumination intensity of 3 Wcm⁻², which is equal to $\approx 2 \times 10^9$ photons per second being absorbed in the reverse-bias part of the CdS NW.

To gain some additional insight into the unusual bias dependence of the depletion layer width, we have also carried out a simple model calculation of the CdS-NW system. We assume a cylindrical NW pn junction, entirely embedded in dielectric and with electrodes much larger than the NW. In such a system the electric field, and hence the carrier distribution, are strongly influenced by the proximity of the surrounding dielectric. The carrier distribution is calculated from a numerical solution to Poisson's equation in cylindrical co-ordinates, obtained with a commercial device simulator.^[17] The details of the simulations are closely similar to those reported previously.^[4] Figure 5A shows the evolution of the electron concentration with reverse bias in the n-type CdS-NW section of a pn heterojunction, with 2×10^{16} cm⁻³ electrons as mobile charge carriers. Figure 5B plots the resulting depletion width versus reverse bias, for various concentrations of mobile charge carriers. Even in this entirely classical picture of a pn junction, there is a strong deviation from the classical square-root junction behavior; instead a clear linear component in the depletion width versus bias is clearly seen. We note that these results are also broadly consistent with electrostatic calculations on carbon-nanotube diodes.^[11] For constant charge distributions, those calculations

show a linear voltage dependence in the limit of depletion widths smaller than the wire diameter. In the opposite limit of depletion widths much larger than the wire diameter, the depletion widths tend to grow exponentially with voltage, as in Reference [11]. We note that the numerical calculations and, more importantly, the experiments indicate a linear voltage dependence of the space-charge layer even at large depletion widths, compared to the nanowire diameter.

These simple models for the PL measurements serve to illustrate clearly that the electrostatics and carrier distribution in a NW pn-junction system are highly unusual; however, they cannot describe in more detail questions related to the intensity dependence of the PL, nor can we ascertain the precise origin of the mobile carriers.

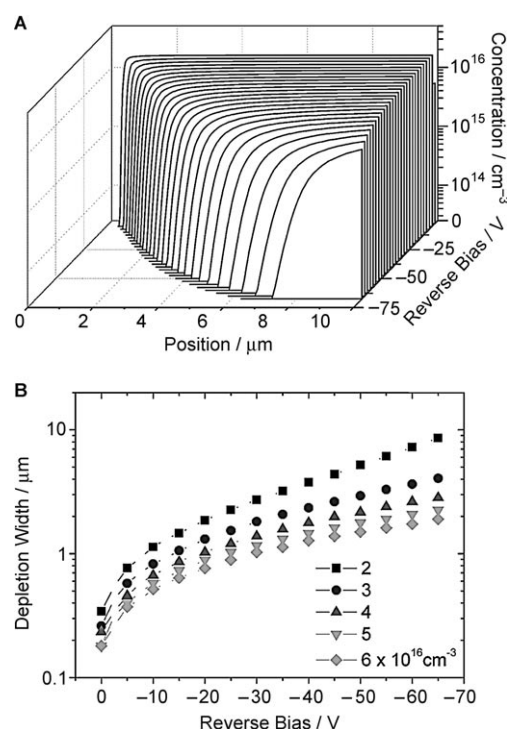


Figure 5. Numerical simulations of the carrier depletion in a fully embedded Si/CdS-NW pn junction. The surrounding medium is assumed to be SiO₂. A) The electron concentration in the n-type CdS section, doped to 2×10^{16} cm⁻³, as a function of reverse bias. B) The depletion width as a function of reverse bias for various doping concentrations.

In summary, a technique to visualize the depletion widths in 1D pn junctions is reported. Our studies of crossed p^+ -Si/n-CdS-NW diodes showed a linear dependence between the reverse bias and the depletion width in CdS NWs indicating a weak screening effect of the junction electric field. The visualization of the depletion widths is a powerful tool for estimates of the carrier distributions and device capacitances. We have also presented 3D electrostatic simulations of a simplified NW heterojunction, and using this simulation show that the carrier depletion widths deviate from the traditional square-root dependence purely due to electrostatic effects. Optical probing of the space-charge region in direct-bandgap semiconducting NWs using our approach should be generally applicable to direct-bandgap materials. More generally, we believe the results from these studies provide further evidence for unique characteristics of NW electronic devices, and highlight the importance of further characterizing their key features in the future.

Experimental Section

Heterostructured diodes were fabricated as reported.^[9,10] Briefly, intrinsic n-type CdS-NWs were crossed with p^+ -SiNWs with a microfluidic directed assembly using orthogonal sequential flows of CdS and Si NW dispersions (ethanol) on thermal oxide (600 nm) covered silicon wafer^[5]. Electron-beam lithography was used to pattern electrodes at the ends of crossed NW structures, and titanium contacts (100 nm) were deposited by electron-beam evaporation.

The devices were cooled to 4.2 K in an optical cryostat. PL experiments were carried out by exciting the NWs using frequency doubled Ti:sapphire laser pulses (≈ 400 nm; repetition rate 76 MHz). PL images from crossed NW diodes were recorded as illustrated schematically in Figure 1A using a home-built epifluorescence microscope ($60\times$, 0.7 NA objective). For length calibration of the NWs electron microscopy images of the diodes were taken to derive the length of the Si and CdS NWs in the PL images.

Keywords:

cadmium sulfide • diodes • nanotechnology • nanowires • silicon

- [1] a) R. S. Wagner, W. C. Ellis, *Appl. Phys. Lett.* **1964**, *4*, 89–90; b) *Highly Anisotropic Crystals* (Ed.: E. I. Givargizov), MSMR: D. Reidel Pub. Co., Dordrecht, The Netherlands, **1987**; c) A. M. Morales, C. M. Lieber, *Science* **1998**, *279*, 208–211.
- [2] O. Hayden, M. T. Björk, H. Schmid, H. Riel, U. Drechsler, S. F. Karg, E. Lörtscher, W. Riess, *Small* **2007**, *3*, 230–234.
- [3] J. A. Appels, H. M. J. Vaes, *IEDM Tech. Dig.* **1979**, 238–241.
- [4] P. Agarwal, M. N. Vijayaraghavan, F. Neuilly, E. Hijzen, G. A. M. Hurkx, *Nano Lett.* **2007**, *7*, 896–899.
- [5] a) A. Bachtold, M. S. Fuhrer, S. Plyasunov, M. Forero, E. H. Anderson, A. Zettl, P. L. McEuen, *Phys. Rev. Lett.* **2000**, *84*, 6082–6085; b) M. S. Gudiksen, L. J. Lauhon, J. Wang, D. C. Smith, C. M. Lieber, *Nature* **2002**, *415*, 617–620.
- [6] a) Y. Gu, E.-S. Kwak, J. L. Lensch, J. E. Allen, T. W. Odom, L. J. Lauhon, *Appl. Phys. Lett.* **2005**, *87*, 043111; b) Y. Ahn, J. Dunning, J. Park, *Nano Lett.* **2005**, *5*, 1367–1370.
- [7] Y. Huang, X. Duan, Q. Wei, C. M. Lieber, *Science* **2001**, *291*, 630–633.
- [8] X. Duan, Y. Huang, Y. Cui, J. Wang, C. M. Lieber, *Nature* **2001**, *409*, 66–69.
- [9] O. Hayden, C. K. Payne, *Angew. Chem.* **2005**, *117*, 1419–1422; *Angew. Chem. Int. Ed.* **2005**, *44*, 1395–1398.
- [10] O. Hayden, R. Agarwal, C. M. Lieber, *Nat. Mater.* **2006**, *5*, 352–356.
- [11] F. Leonard, J. Tersoff, *Phys. Rev. Lett.* **1999**, *83*, 5174–5177.
- [12] a) R. E. Hollingsworth, J. R. Sites, *J. Appl. Phys.* **1982**, *53*, 5357–5358; b) B. Smandek, G. Chmiel, H. Gerischer, *Ber. Bunsen-Ges.* **1989**, *93*, 1094–1103.
- [13] C. Weber, U. Becker, R. Renner, C. Klingshirn, *Cond. Matter* **1988**, *72*, 379–384.
- [14] *Physics of Semiconductor Devices* (Ed.: S. M. Sze), Wiley, New York, **1981**, p. 77.
- [15] a) C. Wiemann, M. Versen, A. D. Wieck, *J. Vac. Sci. Technol. B* **1998**, *16*, 2567–2569; b) A. Sh. Achoyan, A. E. Yesayan, E. M. Kazaryan, S. G. Petrosyan, *Semiconductors* **2002**, *36*, 903–907; c) D. Reuter, C. Werner, A. D. Wieck, S. Petrosyan, *Appl. Phys. Lett.* **2005**, *86*, 162110.
- [16] Y. Civalé, P. Hadley, L. K. Nanver, E. J. G. Goudena, J. Slabbekoorn, Proceedings of 8th Annual Workshop on Semiconductor Advances for Future Electronics and Sensors, *SAFE* **2005**, 79–82.
- [17] Taurus-Medici, version 2006. 10, Synopsis Inc, Mountain View, CA
- [18] It is indeed possible to derive the linear and exponential components from expansions of an appropriate classical dipole potential assuming uniform charge distributions along the wires. This, and the close analogy between our system and the calculations in Ref. [11], was pointed out by one of the peer reviewers.

Received: July 27, 2007

Published online on October 25, 2007